Dynamic Analysis of Interior Permanent Magnet Motor Based on a Magnetic Circuit Model

Kenji Nakamura, Kenichi Saito, and Osamu Ichinokura, *Member, IEEE*

***Abstract*—This paper presents a new magnetic circuit model of an interior permanent magnet (IPM) motor for use in SPICE, which is the general-purpose circuit-simulation program. The magnetic circuit model consists of reluctances and permanent magnet magnetomotive-force sources. In the SPICE simulation, a magnetic circuit model of the IPM motor and its driving circuit are coupled by a proper circuit. Using the proposed model, we can calculate dynamic characteristics of the IPM motor easily.**

***Index Terms*—Dynamic analysis, interior permanent magnet (IPM) motor, magnetic circuit model, SPICE.**

I. Introduction

In recent years, high-efficiency motors are required in public welfare and the industrial field. An interior permanent magnet (IPM) motor has high efficiency and torque because the motor can utilize both magnet and reluctance torque due to the magnetic saliency. The IPM motor is widely used for electric household appliances, OA, and electric vehicles [1], [2].

For the optimum design, several papers have reported on the analysis of the IPM motors based on a finite element method (FEM). Most of the papers, however, discussed static characteristics such as a motor torque and flux distribution [3], [4]. For the dynamic analysis, some papers have reported about an electrical equivalent circuit of the IPM motor [5], [6]. Another effective solution for the dynamic analysis of the IPM motor is utilization of the magnetic circuit model.

This paper presents a new magnetic circuit model of the IPM motor for use on the general-purpose circuit simulation program "SPICE." First, we obtain the magnetic circuit model of the IPM motor based on the fundamental characteristics of the motor. Second, we combine the motor magnetic circuit and its driving circuit using a proper circuit in the SPICE. We also calculate dynamic characteristics of the IPM motor, including the motor-driving circuit.

II. Magnetic Circuit Model

Fig. 1 shows a schematic diagram of the IPM motor used in the considerations. The number of poles of a stator and rotor are 6 and 4, respectively. The stator has windings concentrated around each stator pole. The number of winding turns of each phase is 150. The rare-earth magnet "Nd-Fe-B" is buried in the rotor iron. Residual magnetic flux density B_r and coercive force H_c of the permanent magnet are about 1.3 T and 1000 kA/m, respectively. Fig. 2 is the driving circuit of the IPM motor. In this paper, the rotor angle θ, where the rotor is in the position as shown in Fig. 2, is set to 0°.

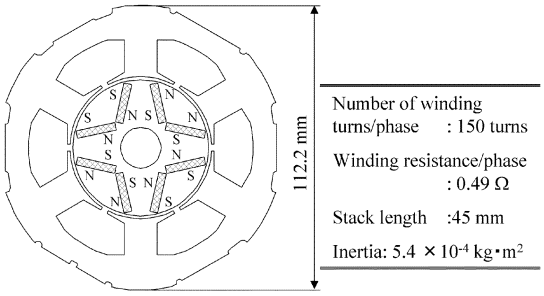

Fig. 1. Schematic diagram of the IPM motor.

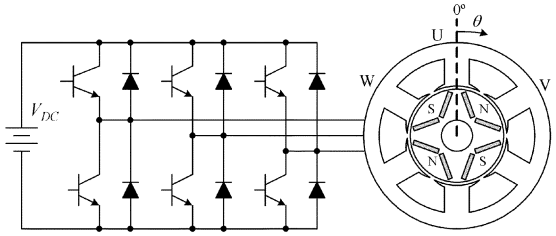

Fig. 2. Configuration of the motor-driving circuit.

The IPM motor utilizes both magnet and reluctnace torques due to the variation of reluctance in the magnetic circuit. Therefore, it is understood that the magnetic circuit model of the IPM motor consists of reluctances and permanent magnet MMF sources.

First, we obtain the reluctances of the magnetic circuit model. We assume that regions of permanent magnet burying in the rotor iron are the vacuum space. When a current flows through the U-phase windings under the assumption, the fluxes flow in the motor as shown in Fig. 3(a). The magnetic circuit of the IPM motor is determined based on the flux flow. If the leakage flux ϕ_l is as small as it can be neglected, then the magnetic circuit corresponding to the flux flow is given as shown in Fig. 3(b). In the figure, the MMF's dependance on the winding currents are Ni_u, Ni_v, and Ni_w, respectively. The variable reluctances between each phase are $R_{uv}(\theta)$ and $R_{wu}(\theta)$, respectively. In this paper, in order to obtain the relationship between the reluctance and rotor angle, we calculate the inductance of stator

Manuscript received January 2, 2002.

K. Nakamura is with the Dept. of Electrical and Communication Engineering, Tohoku University, Aramaki, Aoba-ku, Sendai 980-8579, Japan (e-mail: nakaken@ecei.tohoku.ac.jp).

K. Saito is with the Dept. of Electrical and Communication Engineering, Tohoku University, Aramaki, Aoba-ku, Sendai 980-8579, Japan (e-mail: kenichi@power.ecei.tohoku.ac.jp).

O. Ichinokura is with the Dept. of Electrical and Communication Engineering, Tohoku University, Aramaki, Aoba-ku, Sendai 980-8579, Japan (e-mail: ichinoku@ecei.tohoku.ac.jp).

Digital Object Identifier 10.1109/TMAG.2003.816738

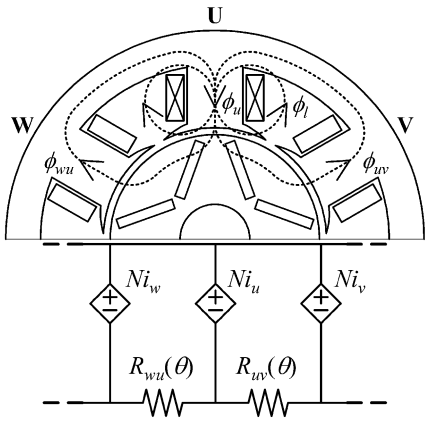

Fig. 3. Flux flow diagram when a current flows through the U-phase windings and the magnetic circuit corresponding to it.

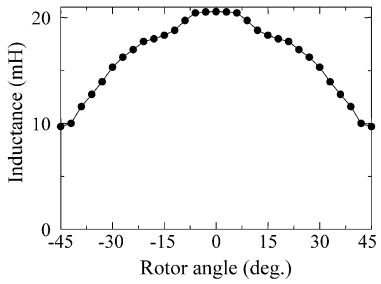

Fig. 4. The U-phase inductance $L_u(\theta)$ versus rotor angle curve.

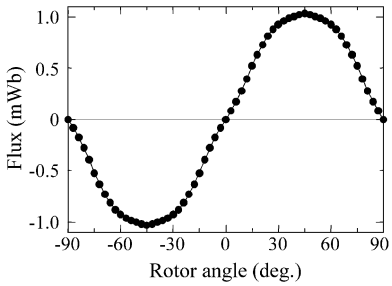

Fig. 5. Variation of flux $\phi_{mu}(\theta)$ passing through the U-phase stator pole with rotor angle.

winding for various rotor angles using a FEM analysis. Fig. 4 is the U-phase winding inductance $L_u(\theta)$ versus rotor angle curve. The inductance curve can be expressed with Fourier series as

$$L_u(\theta) = L_0 + \sum_{k=1}^{n} L_k \cos 4k\theta. \tag{1a}$$

In case of the other phases, the inductances are given in the same manner as the U-phase, which is

$$L_v(\theta) = L_0 + \sum_{k=1}^{n} L_k \cos 4k(\theta - 2\pi/3) \tag{1b}$$

$$L_w(\theta) = L_0 + \sum_{k=1}^{n} L_k \cos 4k(\theta - 4\pi/3). \tag{1c}$$

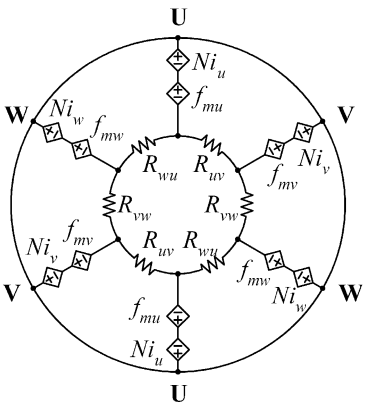

Fig. 6. The magnetic circuit model of the IPM motor.

Mutual inductances M_{uv}, M_{vw}, and M_{wu} are given by

$$M_{uv}(\theta) = \frac{L_0}{2} - \sum_{k=1}^{n} L_k \cos 4k(\theta - 4\pi/3) \tag{2a}$$

$$M_{vw}(\theta) = \frac{L_0}{2} - \sum_{k=1}^{n} L_k \cos 4k\theta \tag{2b}$$

$$M_{wu}(\theta) = \frac{L_0}{2} - \sum_{k=1}^{n} L_k \cos 4k(\theta - 2\pi/3). \tag{2c}$$

When the nonlinearity of core material is neglected, the reluctances are given by the definition of the inductance $L = (N^2/R_m)$, which is

$$R_{uv}(\theta) = \frac{N^2}{M_{uv}}, \quad R_{uv}(\theta) = \frac{N^2}{M_{uv}}, \quad R_{uv}(\theta) = \frac{N^2}{M_{uv}} \tag{3}$$

where the number of winding turns is N.

Next, we determine the permanent magnet MMF sources of the magnetic circuit model. Using the finite-element method (FEM) analysis, we calculate the flux, which flows through the stator pole due to the magnetization of the permanent magnet. Fig. 5 shows the variation of flux $\phi_{mu}(\theta)$ passing through the U-phase stator pole with rotor angle. The flux is expressed as an approximate equation, which is

$$\phi_{mu}(\theta) = \Phi_m \sin 2\theta. \tag{4}$$

The U-phase permanent magnet MMF sources $f_{mu}(\theta)$ are derived by the Ohm's law for magnetic circuits

$$f_{mu}(\theta) = R_{mu}\phi_{mu} = \frac{N^2}{L_u}\phi_{mu}. \tag{5}$$

In case of the other phases, the permanent magnet MMF sources can be obtained as same as the U-phase. Finally, the magnetic circuit model of the IPM motor is expressed as shown in Fig. 6.

III. Dynamic Analysis

Fig. 7 shows a flow diagram of the calculation. In Fig. 7, when the rotor angle θ is given, the controller determines a transistor gate signal and the exciting current in the motor-driving

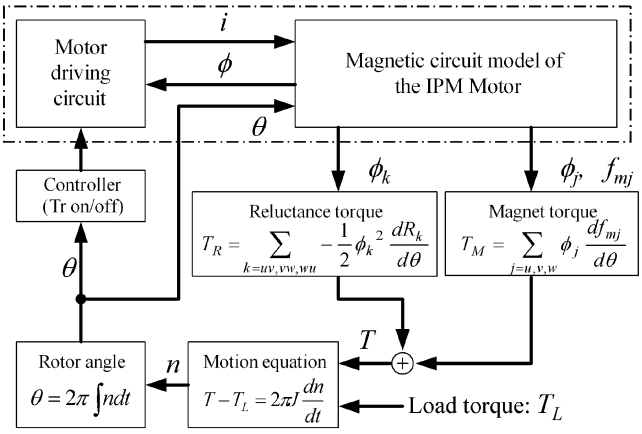

Fig. 7. Flow diagram of the calculations.

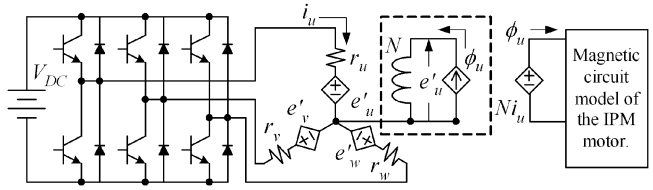

Fig. 8. The electric and magnetic coupled circuit of the IPM motor for the SPICE simulation.

circuit is calculated. From the fluxes in the magnetic circuit model and differential of the reluctance $dR_k(\theta)/d\theta$ and permanent magnet MMF $df_{mk}(\theta)/d\theta$, we obtain a reluctance torque T_R and magnet torque T_M, respectively. When the load torque T_L is given, the rotational speed n is calculated based on motion equation. The integral of rotational speed gives the rotor angle θ.

All above calculations are carried out in the SPICE simulation. The torque, motion equation, rotor position, and controller, as shown in Fig. 7, are expressed by the Analog Behavior Model (ABM), which is one of the standard components of the SPICE. Using the ABM, an element can be expressed freely by an arithmetic expression and a lookup table.

As shown in Fig. 8, the motor driving circuit and magnetic circuit model of the IPM motor are coupled by "flux-voltage" circuit, which is surrounded with a dashed line [7]. Fig. 8 shows only the U-phase "flux-voltage" circuit. In Fig. 8, the winding resistances and induced voltages are r_u, r_v, r_w and e'_u, e'_v, e'_w, respectively. In the SPICE, the MMF source Ni_u is a voltage source controlled by the U-phase current i_u. When the flux ϕ_u in the magnetic circuit is calculated, the induced voltage e'_u is given by "flux-voltage" circuit. The value of inductance is N, which is equal to the number of winding turns.

Based on the calculation model, we compute dynamic characteristics of the IPM motor. Fig. 9 shows the only example of transient characteristics of the IPM motor. The direct-current (dc) source voltage $V_{\rm DC}$ is 280 V. The IPM motor starts with no-load and is applied to a load of 3.0 Nm after 0.15 s. It reveals that we can estimate the dynamic characteristics, including the starting characteristics of the IPM motor using the proposed model. Fig. 10 shows calculated waveforms of the line voltage and phase current when the load torque is 3.0 Nm.

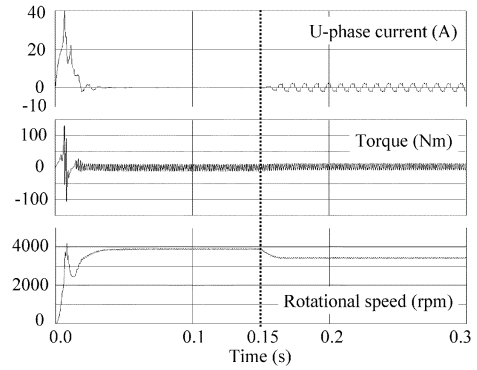

Fig. 9. Transient characteristics of the IPM motor when the motor starts with no-load and is applied to a load of 3.0 Nm after 0.15 s.

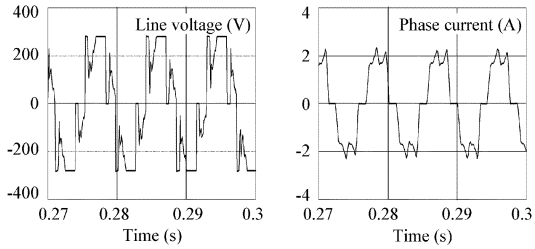

Fig. 10. Calculated waveforms of the line voltage and phase current when the load torque is 3.0 Nm.

IV. Conclusion

We proposed a new magnetic circuit model of the IPM motor for use in SPICE. We can easily calculate the exciting current, torque, and speed. In this paper, we used the FEM analysis to obtain the inductance. If we can obtain the inductance based on the other methods, we can simulate the dynamic operation of the IPM motor without the FEM.

References

[1] J. W. Park, D. H. Koo, J. M. Kim, and H. G. Kim, "Improvement of control characteristics of permanent-magnet synchronous motor for electric vehicle," *IEEE Trans. Ind. Applicat.*, vol. 37, no. 6, pp. 1754–1760, 2001.

[2] Y. Kawase, N. Mimura, and K. Ida, "3-D electromagnetic force analysis of effects of off-center of rotor in interior permanent magnet synchronous motor," *IEEE Trans. Magn.*, vol. 36, no. 4, pp. 1858–1862, 2000.

[3] D. J. Sim, D. H. Cho, J. S. Chun, H. K. Jung, and T. K. Chung, "Efficiency optimization of interior permanent magnet synchronous motor using generic algorithms," *IEEE Trans. Magn.*, vol. 33, no. 2, pp. 1880–1883, 1997.

[4] T. Ohnishi and N. Takahashi, "Optimal design of efficient IPM motor using finite element method," *IEEE Trans. Magn.*, vol. 36, no. 5, pp. 3537–3539, 2000.

[5] T. M. Jahns, G. B. Kliman, and T. W. Neumann, "Interior permanent-magnet synchronous motors for adjustable-speed drives," *IEEE Trans. Ind. Applicat.*, vol. 22, no. 4, pp. 738–747, 1986.

[6] G. H. Kang, J. P. Hong, G. T. Kim, and J. W. Park, "Improved parameter modeling of interior permanent magnet synchronous motor based on finite element analysis," *IEEE Trans. Magn.*, vol. 36, no. 4, pp. 1867–1870, 2000.

[7] O. Ichinokura, S. Suyama, T. Watanabe, and H. J. Guo, "A new calculation model of switched reluctance motor for use on spice," *IEEE Trans. Magn.*, vol. 37, no. 4, pp. 2834–2836, 2001.